Advances in Applied Physics, Vol. 5, 2017, no. 1, 9 - 21
HIKARI Ltd, www.m-hikari.com
https://doi.org/10.12988/aap.2017.711

Excitation Cross-Sections of Singly Charged Zinc Ion in E–Zn Collisions

Yu. M. Smirnov

National Research University «Moscow Power Engineering Institute»
Krasnokazarmennaya str., 14, Moscow, 111250 Russia

Abstract

The method of extended crossing beam with recording of optical signal from the intersection area between the electron and atom beams was used to study excitation of singly-charged zinc ion from the ground state of the zinc atom. Fifty-five ZnII excitation cross sections have been measured at incident electron energy of 30 eV. Seven optical excitation functions (OEFs) have been recorded in the electron energy range E = 0–200 eV. The results obtained have been compared with findings from past experiments.

Keywords: Singly charged Zinc ion, E–Zn collisions

1 Introduction

A metal with a remarkably high saturated vapor pressure at temperatures as low as T < 1000 K, vaporized zinc was among the first choices for active media in laser generation. By the time a survey of metal-vapor ion lasers was published in 1990 [7], generation experiments had been tried successfully for a total of 17 transitions of the singly-charged zinc ion. ZnII generation lines lie within the wavelength range λ = 491.16 – 5084.8 nm disposed in both visible-light and IR spectrum range. Experiments cited relied on various discharge types in addition to electron-impact pumping without the use of a buffer gas [12].

Hollow-cathode discharge is an effective method of obtaining inverse population. “Bombardment of the cathode surface with ions, high-velocity neutral particles and photons produces emission of secondary electrons that then accelerate in the dark cathode area and produce an electron beam with energy of

300–400 eV. Within the discharge, these high-velocity electrons are effective at ionizing atoms, creating a suitable active medium for ion lasers" [10, P. 7]. However the electron gun has proved itself more effective: "Rocca et al. [11] have proposed and implemented… a new method for excitation of continuous-action ion lasers with DC electron beams. To that end they have devised glow-discharge electron guns… capable of producing highly collimated electron beams with energies ranging between 1 and 10 kV and currents as high as 1.2 A. Glow-discharge electron guns operate in helium media with pressures up to 3 Torr while needing no differential pumping. Electron beam generation efficiency reached 80%. These results surpass the performance of hollow-cathode discharge by an order of magnitude" [10, P. 15]. Thus electron-atom collisions play a major role in processes producing inverse population in metal-vapor lasers.

As zinc is an easily vaporizable element, experimental study of electron collisions with zinc atoms is not a particularly daunting task. In [2], the vapor-filled cell method was used to study excitation of five ZnII spectral lines from the ground state of the zinc atom in a single electron-atom collision (excitation with simultaneous single ionization). Five cross-section values have been determined at incident electron energy of 200 eV and three optical excitation functions (OEFs) have been recorded in the electron energy range E = 0–260 eV. Coming on the heels of [2], another study [1] used the same method and reported on five cross-section values measured at OEF maxima as well as four OEFs recorded in the electron energy range E = 0–250 eV. Notably, lines λ = 492.389/401 and 589.436 nm have been surveyed both in [2] and in [1].

A report on eight ZnII excitation cross-sections measured at incident electron energy E = 60 eV followed up shortly [9]. In turn it was followed by the most extensive study of ZnII excitation to date [6] where instrument sensitivity was increased greatly as a result of applying the photon count technique. Furthermore, [6] assesses the quality of OEF shape data in [6] and previous papers as fair even whilst absolute cross-section values are 3 to 4 times distinguished. Thus, determination of absolute cross-section values remains the main problem when measuring excitation cross-sections of the singly-charged zinc ion.

This paper uses the method of extended crossing beams to obtain more detailed information on ZnII excitation from the ground level of the zinc atom, $4s^2\ ^1S_0$.

2 Main Experimental Conditions

Considering that the method of extended crossing beams was discussed extensively in a number of past publications (e.g. [14, 15]), it would be unnecessary to describe it in detail in this paper. We will only note some basic conditions concerning to the zinc atom experiment proper.

The atom beam was generated by vaporizing 99.999% pure zinc from a tantalum crucible that had its outer surface heated with an electron-gun ray. Due to its saturated vapor pressure of 10 Pa at the melting temperature, zinc turned to vapor directly from solid phase. Transverse dimensions of the atom beam were

limited to 26 × 200 mm at its intersection zone with electron beam by a series of three apertures cooled with running water. Zinc atom concentration in the beam crossing area read 1.7×10^{10} cm^{-3}. Due to an energy interval $\Delta E \geq 32500$ cm^{-1} separating lower excited zinc atom levels from the ground level, thermal population at these excited levels is negligible and all atoms in the beam remain in their ground state $4s^2\,{}^1S_0$ before colliding with electrons.

Electron beam current density across the entire electron energy working range of E = 0–200 eV stood below 1.0 mA/cm^2. The setup had a real spectral resolution of about 0.1 nm within the short-wave part of a spectrum at $\lambda < 600$ nm, deteriorating to ~0.2 nm at $\lambda > 600$ nm as the monochromator diffraction grating had to be replaced. Considering that measured ZnII excitation cross-section values were rather small, error in their relative values ranged 8–15%. Absolute excitation cross-section values have been determined with a margin of error ranging 28–35%. [13] discuss major sources of error in extended-beam experiments in detail.

3 Results and Discussion

Fifty-five spectral lines have been identified as belonging to the ZnII spectrum on spectrograms recorded with incident electron energy of 30 eV in wavelength range λ = 190–780 nm. Seven optical excitation functions (OEFs) have been recorded with electron energies E varying between 0 and 200 eV.

Findings from measurements supplemented with necessary reference spectroscopic data are summarized in Table 1 (lines having OEFs recorded) and Table 2 (lines for which reliable recording of OEFs proved impossible). Table 1

Table 1. Cross-Sections of Singly-Charged Zinc Ion (Simultaneous Excitation and Ionization)

λ nm	Transition	J_{low}–J_{up}	E_{low} cm^{-1}	E_{up} cm^{-1}	Q_{30} 10^{-18} cm^2	Q_{max} 10^{-18} cm^2	$E(Q_{max})$ eV	OEF
202.548	$4s^2S$–$4p^2P°$	1/2–3/2	0	49355	71.0	102.	50	*3*
206.200	$4s^2S$–$4p^2P°$	1/2–1/2	0	48481	44.5	65.7	50	*2*
250.199	$4p^2P°$–$5s^2S$	1/2–1/2	48481	88437	3.30	3.83	36	*1*
255.795	$4p^2P°$–$5s^2S$	3/2–1/2	49355	88437	6.29	7.30	36	*1*
491.163[1]	$4d^2D$–$4f^2F°$	3/2–5/2	96909	117264	0.36	0.69	40	*4*
492.389 492.401[1]	$4d^2D$–$4f^2F°$ $4d^2D$–$4f^2F°$	5/2–5/2 5/2–7/2	96960 96960	117264 117263	} 0.52	0.94	38	*5*
589.436[1]	$4p^2P°$–$4s^2\,{}^2D$	1/2–3/2	48481	65441	15.8	29.8	100	*6*
621.458[1]	$4p^2P°$–$4s^2\,{}^2D$	3/2–3/2	49355	65441	2.16	4.07	100	*6*
747.877[1]	$4p^2P°$–$4s^2\,{}^2D$	3/2–5/2	49355	62722	27.6	58.6	100	*7*

indicates wavelengths λ, transitions (with an abbreviated notation 4*p*' used for terms belonging to $3d^9 4s4p$ configurations), internal quantum numbers for the lower J_{low} and upper J_{up} levels, energies of the lower E_{low} and upper E_{up} levels, excitation cross-sections at incident electron energy of 30 eV Q_{30} and at the OEF maximum Q_{max}, and the position of the maximum $E(Q_{max})$. The OEF column indicates curve numbers in accordance with their numbering in Fig. 1. Table 2 differs from Table 1 by having the three final columns omitted. Most wavelength

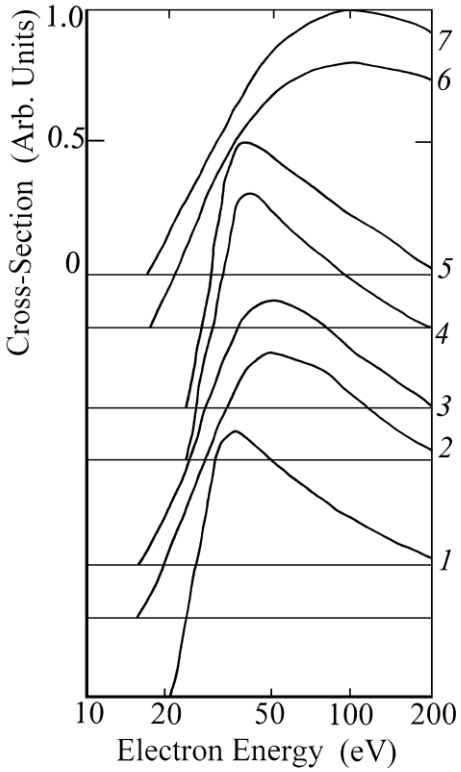

Figure 1: Optical excitation functions of singly-charged zinc ion.

Table 2. Cross-Sections of One-Charged Zinc Ion (Simultaneous Excitation and Ionization)

λ nm	Transition	J_{low}–J_{up}	E_{low} cm^{-1}	E_{up} cm^{-1}	Q_{30} 10^{-18} cm^2
1	2	3	4	5	6
191.481	$4p'\ ^2F°–5s'\ ^4D$	5/2–3/2	110672	162897	0.10
194.041	$4p'\ ^4D°–5s'\ ^4D$	1/2–1/2	112534	164070	0.079
194.846	$4s^2\ ^2D–4p'\ ^2D°$	5/2–3/2	62722	114045	0.062
195.298	$4p'\ ^4D°–5s'\ ^4D$	7/2–5/2	110867	162070	0.11
196.451	$4p'\ ^4D°–5s'\ ^4D$	3/2–3/2	111994	162897	0.12
196.939	$4s^2\ ^2D–4p'\ ^2P°$	5/2–3/2	62722	113499	0.13

Table 2. (Continued): Cross-Sections of One-Charged Zinc Ion (Simultaneous Excitation and Ionization)

198.209	$4p'\ ^4D°–5s'\ ^4D$	7/2–7/2	110867	161318	0.14
198.696	$4p'\ ^4D°–5s'\ ^4D$	5/2–5/2	111743	162070	0.15
201.645	$4p'\ ^4D°–5s'\ ^4D$	5/2–7/2	111743	161318	0.046
203.931	$4s^2\ ^2D–4p'\ ^4D°$	5/2–5/2	62722	111743	1.97
1	2	3	4	5	6
205.676	$4s^2\ ^2D–4p'\ ^2D°$	3/2–3/2	65441	114045	0.16
206.423	$4p^2P°–4d^2D$	1/2–3/2	48481	96909	2.14
209.993	$4p^2P°–4d^2D$	3/2–5/2	49355	96960	4.22
210.217	$4p^2P°–4d^2D$	3/2–3/2	49355	96909	0.67
212.274	$4s^2\ ^2D–4p'\ ^4D°$	3/2–1/2	65441	112534	0.19
234.668	$4s^2\ ^2D–4p'\ ^4P°$	5/2–3/2	62722	105322	0.11
238.392	$5s^2S–4p''\ ^2P°$	1/2–3/2	88437	130371	0.17
239.004	$4s^2\ ^2D–4p'\ ^4F°$	3/2–5/2	65441	107268	0.53
243.274	$4d^2D–8f^2F°$	3/2–5/2	96909	138003	0.094
243.576	$4d^2D–8f^2F°$	5/2–7/2	96960	138002	0.15
243.953	$4s^2\ ^2D–4p'\ ^4P°$	5/2–5/2	62722	103701	0.087
250.669	$4s^2\ ^2D–4p'\ ^4P°$	3/2–3/2	65441	105322	0.038
256.446	$4d^2D–7f^2F°$	3/2–5/2	96909	135892	0.14
257.065	$4s^2\ ^2D–5p^2P°$	5/2–3/2	62722	101611	0.25
276.392	$4s^2\ ^2D–5p^2P°$	3/2–3/2	65441	101611	0.054
278.281	$4s^2\ ^2D–5p^2P°$	3/2–1/2	65441	101366	0.13
293.534	$5p^2P°–9s^2S$	1/2–1/2	101366	135423	0.031
295.669	$5p^2P°–9s^2S$	3/2–1/2	101611	135423	0.046
329.942	$4d^2D–5f^2F°$	3/2–5/2	96909	127209	0.21
330.601	$4d^2D–5f^2F°$	5/2–7/2	96960	127199	0.32
380.638	$5p^2P°–6d^2D$	1/2–3/2	101366	127630	0.10
384.029	$5p^2P°–6d^2D$	3/2–5/2	101611	127643	0.17
384.223	$5p^2P°–6d^2D$	3/2–3/2	101611	127630	0.038
407.813	$5p^2P°–7s^2S$	1/2–1/2	101366	125880	0.092
411.939	$5p^2P°–7s^2S$	3/2–1/2	101611	125880	0.195
414.861	$5s^2S–4p'\ ^4D°$	1/2–1/2	88437	112534	0.072
535.747	$4f^2F°–7g^2G$	7/2–7/2,9/2	117263	135923	} 0.26
535.766	$4f^2F°–7g^2G$	5/2–7/2	117264	135923	
602.119[1]	$5p^2P°–5d^2D$	1/2–3/2	101366	117969	0.62
610.249[1]	$5p^2P°–5d^2D$	3/2–5/2	101611	117993	1.20
611.156	$5p^2P°–5d^2D$	3/2–3/2	101611	117969	0.094
648.301	$4f^2F°–6g^2G$	7/2–7/2,9/2	117263	132683	} 0.35
648.327	$4f^2F°–6g^2G$	5/2–7/2	117264	132683	
758.846[1]	$5s^2S–5p^2P°$	1/2–3/2	88437	101611	1.56
773.249[1]	$5s^2S–5p^2P°$	1/2–1/2	88437	101366	1.07

and energy level values have been sourced from [3]. More precise values of λ are provided for 15 spectral lines in [5] even though the discrepancy between [3] and [5] never exceeds 0.04 nm. Energy values from [3, 5] differ by less than 2 cm^{-1}; [5] provides refined values of *E* for eleven low-lying levels.

Fig. 2 shows a state diagram for a singly-charged zinc ion with transitions surveyed by us. Terms are shown without *J*-split with the exception of the lower even term $3d^9 4s^2\ ^2D$ having $\Delta E > 1000$ cm^{-1}. Principal quantum number values are shown next to terms belonging to configurations with ten 3*d* electrons (on the left side of the plot). Odd terms belonging to $3d^9 4s4p$ configurations are indicated in the plot area. Some of relatively low-lying terms are not shown in Fig. 2 as allowed transitions they give rise to are out of the spectral range of our setup, such as the transitions $5p^2P°$–$6s^2S$ (faint lines near λ ~ 760 nm), $4p^2P°$–$6s^2S$ (in the vacuum-UV part of the spectrum), $4f^2F°$–$5g^2G$ (in the IR part of the spectrum) etc.

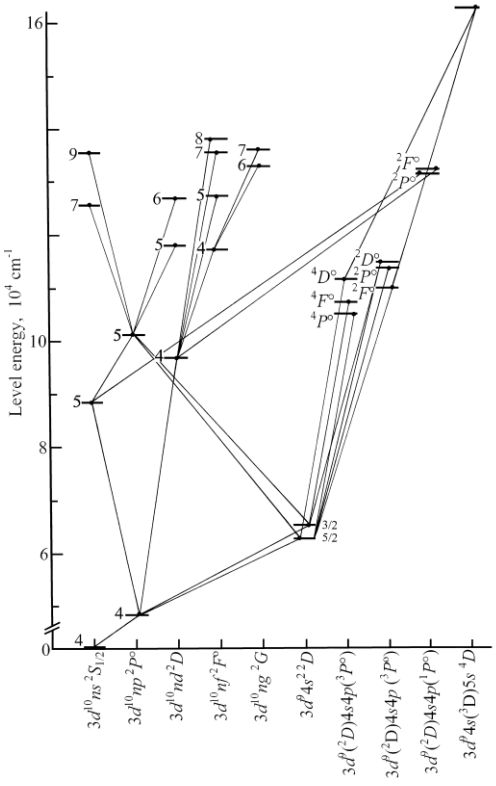

Figure 2: Partial state diagram of ZnII with transitions investigated.

Recorded transitions from $np^2P°$ levels are conspicuously absent at *n* = 6,7,8. The relatively intense transitions from $6p^2P°$ levels (λ ≈ 317 nm) were blended in our experiment with hydroxyl molecular bands as there were some water

molecules among residual gases in the vacuum chamber. As for $7,8p^2P°$ levels, strong perturbation by $3d^9(^2D)4s4p(^1P°)\ ^2P°$ levels take place [8, Appendix]. The nature of this perturbation is evident in Fig. 3 as reproduced from [8]. "A graph of the Rydberg denominators of these series led us to conclude that $7p^2P°$ is perturbed by the upper $^2P°$ term of $3d^9 4s4p$ (Fig. 3), and that similar interactions must depress $8p^2P°_{1/2}$ and push $8p^2P°_{3/2}$ upward" [8, P. 1279].

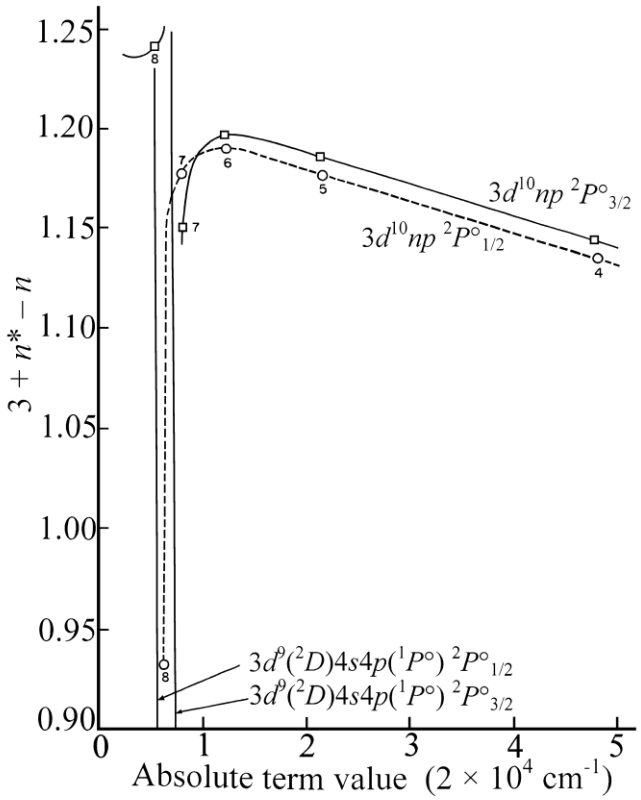

Figure 3: "The $^2P°$ series in ZnII. The value of the principal quantum number n is given near the point for each member. The absolute term values are taken with respect to the $3d^{10}$ limit, 144891 cm^{-1} above the ground level of ZnII. The quantity n^* was determined from the relation, $(n^*)^2 \times$ (abscissa) = 109737.3 cm^{-1}, the Rydberg constant" [8].

It would be instructive to compare our findings with data from past experiments. "The Q_{ij} were measured for some lines…: for two lines by Anderson (1970), three lines by Aleinikov and Ushakov (1970) and eight lines by Penkin *et al* (1972). The shapes of their optical excitation functions agree qualitatively with the present ones. On the other hand, the absolute values of the Q_{ij} measured by the present experiment are about four times as large as those measured by Penkin *et al* (1972) and are three times as large as those by Anderson (1970). Those obtained by Aleinikov and Ushakov (1970) are two or three times as large as present ones" [6, P. 1374–1375]. However the assertion of a good agreement between OEF shapes

in [6] and works listed above is questionable for a number of reasons: 1). [2, Table I] provides cross-section values for five ZnII lines at electron energy of 200 eV. Two of them, λ = 250.199 and 255.795 nm, are transitions from a common upper level, $5s^2S_{1/2}$. OEFs for these two lines differ noticeably in [6]. Also different are Q_{200} cross-section values (in 10^{-18} cm^2 units): 0.28 and 0.38 in [2] vs. 0.7 and 1.1 in [6]. 2). Lines λ = 491.163 and 492.401 nm are present in both papers but no OEF is reported for them in [6]. 3). An OEF is provided [2] for the line λ = 610.249 nm (the transition $5p^2P°_{3/2}$–$5d^2D_{5/2}$) which has $Q_{200} = 0.6 \times 10^{-20}$ cm^2. To the contrary, [6] presents no OEF for this line despite its cross-section value being $Q_{50} = 171 \times 10^{-20}$ cm^2 – almost 300 times greater than in [2]. Even though Q_{50} is expectedly greater Q_{200} for all ZnII lines, the difference is modest for the λ = 610.249 nm line (~25%). 4). Lines λ = 589.436 and 621.458 nm would be expected to have identical OEFs, as they have the same upper level $4s^2\ ^2D_{3/2}$. Yet, OEFs reported for these two lines in [1] differ noticeably.

OEFs obtained in our study are in a good agreement with the data from [6], although λ = 589.436 nm shows a discrepancy between $E(Q_{max})$ = 100 eV in our study vs. ≈130 eV in [6]. However this maximum appears flat and rather broad in both studies, its true location thus becoming unclear.

All works cited present findings in different formats turning comparison of absolute cross-section values into a challenge. With tabulated cross-section values referring to electron energies E = 30, 50, 60, 200 eV or in the OEF maximum (besides just a fraction of tabulated cross-sections has OEFs recorded), a further hindrance is posed by OEFs *per se* as they tend to be of minor scale and fall short of producing accurate numerical readings.

Table 3 compares findings from our study with previous researcher's data. It would be most instructive to compare our data with the results from [6] which provides the greatest body of experimental matter. The ratio Q_{30}[P.p.]/Q_{30}[6] ranges between 1.08 and 3.30, with extreme values being unreliable as they correspond to the least intense lines in [6]. For the six remaining lines, the ratio Q_{30}[P.p.]/Q_{30}[6] is in the range 1.24–2.42. It should be noted that the spectral sensitivity of the experimental setup in [6] was determined using reference intensity sources: a standard lamp with a tungsten glow body at λ = 300–600 nm and a deuterium lamp at λ = 190–400 nm. An absorption technique was used in [6] to determine atom concentration in the beam: "The value of N_{Zn} was obtained by measuring the absorption coefficient of the ZnI 307.6 nm line with an absorption method. …In this procedure, we used the value of 5.0×10^4 s^{-1} as the transition probability of the 307.6 nm line…, which has a direct effect upon the value of N_{Zn}. Therefore, when a more accurate value of the transition probability is obtained in the future, N_{Zn} must be modified by the same factor" [6, P. 1373]. The value was refined recently as $A_{ij}(307.6) = 3.3 \times 10^4$ s^{-1} in a compilation paper [16]. A detailed procedure for determining the scale of absolute cross-section values in experiments with extended crossing beams is provided in [14].

Unfortunately neither [6] nor other works by the same authors provide any data on the spectral resolution of their setup. In a paper dedicated to cadmium [4], monochromator dispersion is reported as 3 nm/mm, however there is no indication

of slit width anywhere in the text. Considering that paired lines 210.0/2 and 384.03/23 nm are unresolved in [6, Table 1 and Fig. 3], the spectral resolution must be *a priori* worse than 0.2 nm. Such uncertainty invites several questions: 1). How was it possible to resolve the lines grouped at λ = 329.94 and 330.48/60 nm if there is a pair of much more intense zinc atom lines λ = 330.259/294 nm in between? 2). [6, Table 1] reports a line λ = 248.46 nm (the transition $5s^2S_{1/2}$–$7p^2P°_{3/2}$). However λ = 250.511 nm corresponds to this transition while λ = 248.46 nm could not be classified within existing ZnII level system. Moreover, a line with this wavelength is absent from the most detailed spectroscopic study [3]. 3). Line λ = 384.23 nm is indicated in [6] as the transition $5p^2P°_{1/2}$–$6d^2D_{3/2}$. Indeed λ = 384.23 nm corresponds to the transition $5p^2P°_{3/2}$–$6d^2D_{3/2}$, and the wavelength of the transition $5p^2P°_{1/2}$–$6d^2D_{3/2}$ is λ = 380.634 nm. 4). A transition $4d^2D_{5/2}$–$6f^2F°_{5/2}$ (λ = 280.473 nm) is cited in [6]. Essentially more intense transitions, $4d^2D_{3/2}$–$6f^2F°_{5/2}$ (λ = 280.074 nm) and $4d^2D_{5/2}$–$6f^2F°_{7/2}$ (λ = 280.196 nm), originate in the same multiplet however they are blended with zinc atom lines λ = 280.087/106/117 nm whose intensity exceeds that of ionic lines by almost two orders of magnitude. How was it possible to identify the weakest line of $4d^2D$–$6f^2F°$ multiplet (λ = 280.473 nm) by Δλ > 0.2 nm spectral resolution?

4 Conclusion

The existing body of experimental data on cross-sections of singly-charged zinc ion excited from the zinc atom ground level was supplemented and refined significantly using the method of extended crossing beams. Lines studied include nine laser transitions in the λ = 491–773 nm wavelength range. The obtained cross-section values may be used to creation mathematical models of hollow-cathode discharge and transverse HF discharge lasers.

References

[1] V. S. Aleynikov and V. V. Ushakov, Measurement of Excitation Functions and excitation Cross-Sections of the Zn II and Cd II Spark Lines, *Optics and Spectroscopy*, **29** (1970), 111–112.

[2] R. J. Anderson and E. T. P. Lee, Optical Ionization-Excitation Functions of Zinc, Cadmium, and Mercury by Electron Impact, *The Journal of Chemical Physics*, **53** (1970), 754–759. https://doi.org/10.1063/1.1674054

[3] A. M. Crooker and K. A. Dick, Extensions to the spark spectra of Zinc. I. Zinc II and Zinc IV, *Canadian Journal of Physics*, **46** (1968), 1241–1251. https://doi.org/10.1139/p68-158

[4] T. Goto, K. Hane, M. Okuda and S. Hattori, Direct-Excitation cross-sections for Cd II low-lying excited states by single-electron impact on Cd atoms, *Physical*

Review A, **27** (1983), 1844–1850. https://doi.org/10.1103/physreva.27.1844

[5] D. Gullberg and U. Litzen, Accurately Measured Wavelengths of Zn I and Zn II Lines of Astrophysical Interest, *Physica Scripta*, **61** (2000), 652–656. https://doi.org/10.1238/physica.regular.061a00652

[6] S. Inaba, K. Hane and T. Goto, Direct excitation cross-sections of Zn II states excited by electron–Zn-atom collisions, *Journal of Physics B: Atomic and Molecular Physics*, **19** (1986), 1371–1376. https://doi.org/10.1088/0022-3700/19/9/017

[7] I. G. Ivanov, E. L. Latush and M. F. Sem, *Ionic Lasers on the Metal Vapor*, Energoatomizdat, Moscow, 1990.

[8] W. C. Martin and J. Sugar, Perturbations and Coupling in the d^9sp Configurations of Cu I, Zn II, Ag I, Cd II, and Tl III, *Journal of the Optical Society of America*, **59** (1969), 1266–1280. https://doi.org/10.1364/josa.59.001266

[9] N. P. Penkin, A. A. Mitiureva and E. R. Zhezherina, Effective Cross-Sections for the Excited Zinc Ion Generation under Zinc Atom Ionization by Electron Impact, *Optics and Spectroscopy*, **33** (1972), 567–568.

[10] J. J. Rocca and G. J. Collins, Ultraviolet ionic lasers, *Avtometriya*, (1984), no. 1, 3–19. (in Russian)

[11] J. J. Rocca, J. D. Meyer and G. J. Collins, Hollow cathode electron gun for the excitation of cw lasers, *Physics Letters A*, **87** (1982), 237–239. https://doi.org/10.1016/0375-9601(82)90012-3

[12] M. F. Sem and V. S. Mikhalevski, Pulsed Generation on the Zinc and Cadmium Transitions, *Journal of Applied Spectroscopy* (Minsk), **6** (1967), 668–669.

[13] Yu. M. Smirnov, Excitation cross-sections of the praseodymium atom, *Journal of Physics II France*, **4** (1994), 23–35. https://doi.org/10.1051/jp2:1994113

[14] Yu. M. Smirnov, Excitation of gallium one-charged ion in e–Ga collisions, *Journal of Physics B: Atomic, Molecular and Optical Physics*, **48** (2015), 165204. https://doi.org/10.1088/0953-4075/48/16/165204

[15] Yu. M. Smirnov, TIII excitation cross-sections in collisions of slow electrons with thallium atoms, *Journal of Physics B: Atomic, Molecular and Optical Physics*, **49** (2016), 175204. https://doi.org/10.1088/0953-4075/49/17/175204

[16] W. L. Wiese and G. A. Martin, Transition Probabilities, in *Wavelengths and Transition Probabilities of Atoms and Atomic Ions*, National Standard Reference Data Series, NSRDS–68, National Bureau of Standards, US, 1980, 359–406. https://doi.org/10.6028/nbs.nsrds.68

Received: January 21, 2017; Published: February 14, 2017

Table 3. Comparison of Cross-Section Data of One-Charged Zinc Ion (Simultaneous Excitation and Ionization)

λ	Transition	J_{low}–J_{up}	E_{low}	E_{up}	Q_{30} [P.p.]	Q_{30} [8]	Q_{50} [5]	Q_{50} [8]	Q_{60} [7]	Q_{max} [P.p.]	Q_{max} [6]	Q_{max} [8]
nm			cm^{-1}	cm^{-1}				10^{-18}	cm^2			
202.548	$4s^2S$–$4p^2P°$	1/2–3/2	0	49355	71.0	57.		63.	15.	102.		64.
203.931	$4s^2\,^2D$–$4p'\,^4D°$	5/2–5/2	62722	111743	1.97			0.40				
206.200	$4s^2S$–$4p^2P°$	1/2–1/2	0	48481	44.5	36.		39.	10.	65.7		39.
209.993	$4p^2P°$–$4d^2D$	3/2–5/2	49355	96960	4.22	} 2.8		3.2	1.2			3.3
210.217	$4p^2P°$–$4d^2D$	3/2–3/2	49355	96909	0.67							
234.668	$4s^2\,^2D$–$4p'\,^4P°$	5/2–3/2	62722	105322	0.11			0.037				
239.004	$4s^2\,^2D$–$4p'\,^4F°$	3/2–5/2	65441	107268	0.53			0.20				
250.199	$4p^2P°$–$5s^2S$	1/2–1/2	48481	88437	3.30	1.0	0.58	1.45	0.4	3.83		1.45
255.795	$4p^2P°$–$5s^2S$	3/2–1/2	49355	88437	6.29	2.6	0.79	3.1	0.7	7.30		3.1
276.392	$4s^2\,^2D$–$5p^2P°$	3/2–3/2	65441	101611	0.054			0.0059				
278.281	$4s^2\,^2D$–$5p^2P°$	3/2–1/2	65441	101366	0.13			0.0091				
293.534	$5p^2P°$–$9s^2S$	1/2–1/2	101366	135423	0.031			0.010				
295.669	$5p^2P°$–$9s^2S$	3/2–1/2	101611	135423	0.046			0.011				
329.942	$4d^2D$–$5f^2F°$	3/2–5/2	96909	127209	0.21			0.19				
330.601	$4d^2D$–$5f^2F°$	5/2–7/2	96960	127199	0.32			0.16				
380.638	$5p^2P°$–$6d^2D$	1/2–3/2	101366	127630	0.10			0.041				
384.029	$5p^2P°$–$6d^2D$	3/2–5/2	101611	127643	0.17	} 0.061						
384.223	$5p^2P°$–$6d^2D$	3/2–3/2	101611	127630	0.038							
407.813	$5p^2P°$–$7s^2S$	1/2–1/2	101366	125880	0.092			0.057				
411.938	$5p^2P°$–$7s^2S$	3/2–1/2	101611	125880	0.195			0.14				
491.163[1]	$4d^2D$–$4f^2F°$	3/2–5/2	96909	117264	0.36		0.32	0.26		0.69	1.5	

Table 3. (Continued): Comparison of Cross-Section Data of One-Charged Zinc Ion (Simultaneous Excitation and Ionization)

492.389 492.401[1]	$4d^2D$–$4f^2F°$ $4d^2D$–$4f^2F°$	5/2–5/2 5/2–7/2	96960 96960	117264 117263	}0.52		}0.39	}0.38		}0.94	}2.0	
589.436[1]	$4p^2P°$–$4s^2\,^2D$	1/2–3/2	48481	65441	15.8	11.		17.	5.0	29.8	28.0	21.
602.119[1]	$5p^2P°$–$5d^2D$	1/2–3/2	101366	117969	0.62			0.91				
610.249[1]	$5p^2P°$–$5d^2D$	3/2–5/2	101611	117993	1.20			1.71				
611.156	$5p^2P°$–$5d^2D$	3/2–3/2	101611	117969	0.094			0.59				
621.458[1]	$4p^2P°$–$4s^2\,^2D$	3/2–3/2	49355	65441	2.16	~2		~3	0.8	4.07	7.0	~3.5
747.877[1]	$4p^2P°$–$4s^2\,^2D$	3/2–5/2	49355	62722	27.6	20.		26.	6.2	58.6	65.0	30.
758.846[1]	$5s^2S$–$5p^2P°$	1/2–3/2	88437	101611	1.56			1.35				
773.249[1]	$5s^2S$–$5p^2P°$	1/2–1/2	88437	101366	1.07			0.31				